Vol. 2 • No. 11 • November 2021

ADVANCED PHOTONICS RESEARCH

Open Access

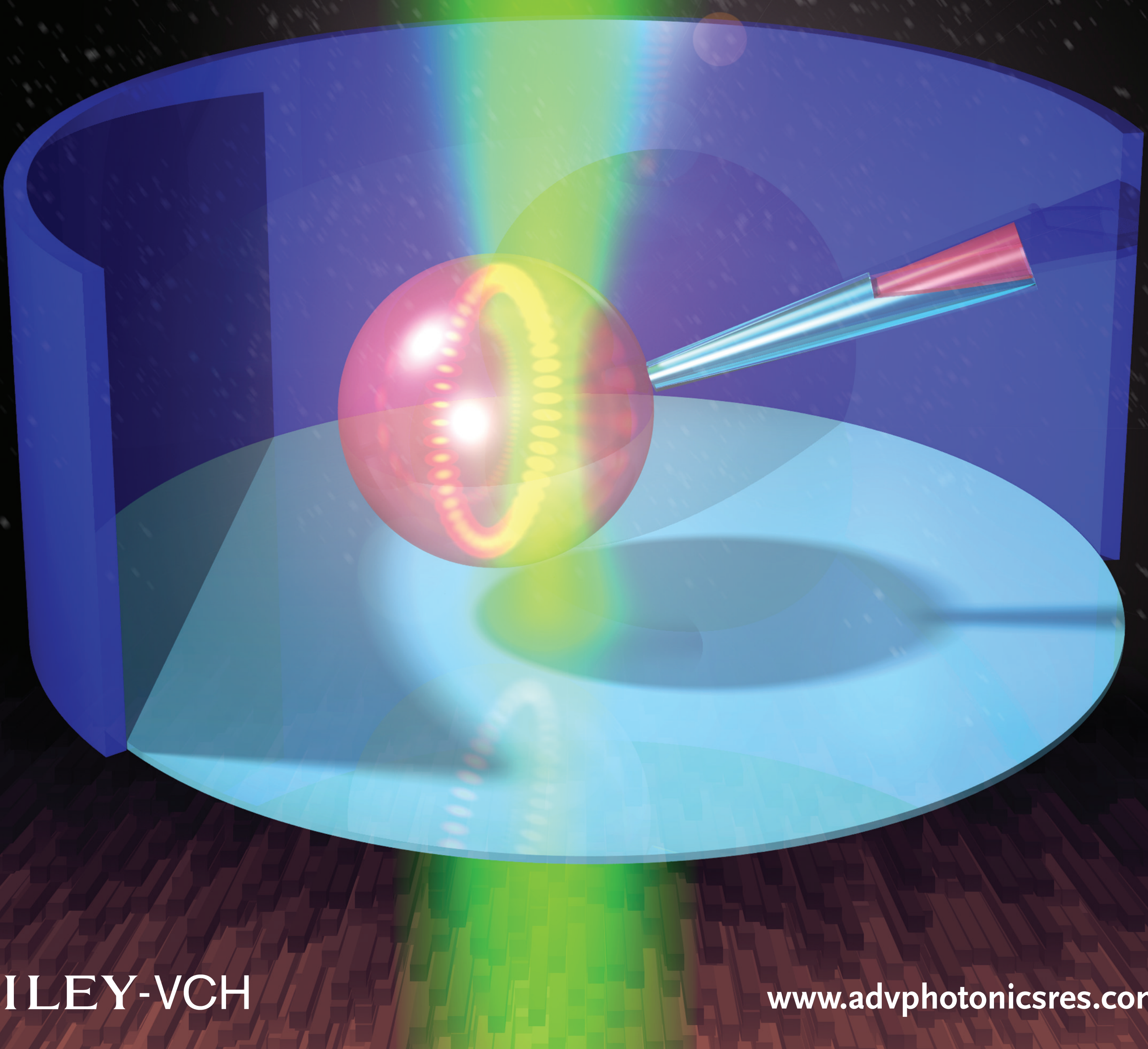

WILEY-VCH

www.advphotonicsres.com

Whispering Gallery-Mode Microdroplet Tensiometry

*Gregor Pirnat and Matjaž Humar**

Droplets are ideally suited to support high-Q-factor whispering gallery modes (WGMs) due to their perfectly smooth surface. WGMs enable extremely precise measurements of the droplet properties such as size and shape. Herein, a simple, fast, and very precise technique to measure interfacial tension (IFT) between two immiscible liquids based on WGMs is demonstrated. A microdroplet is generated at the end of a glass microcapillary, submerged in a continuous liquid phase, and its size changes are monitored with nanometer precision via WGMs, while simultaneously applying finely tunable pressure through the microcapillary. IFT is determined from the size of the droplet and the pressure in the microcapillary at equilibrium. Droplets as small as 8 μm are used, thus requiring extremely small sample volume. The IFT measurements can be carried out also at nonequilibrium state when either the size of the droplet or the chemical composition of the continuous phase changes in time. Simultaneously, the WGMs enable very precise measurement of the refractive index of either the droplet or the continuous phase.

1. Introduction

The interfacial surface tension (IFT) is a crucial quantity in fundamental interfacial science, as well as extremely important for a wide variety of applications ranging from biology, food, pharmaceuticals, cosmetics, to fossil fuel industries.[1–4] Due to the importance of the IFT, numerous tensiometric techniques have been developed to date. The IFT can be measured by probing the elastic energy of the interface by inducing interface deformation, such as in the case of the pendant drop,[5–7] spinning drop,[8,9] microcapillary aspiration methods,[10–13] and others.[14–17] The IFT can also be probed by directly measuring pressure difference across the interface, such as the maximum droplet pressure and growing droplet method.[18,19] Most methods rely on imaging to determine the shape of the interface, which requires a calibrated imaging system, flat optical window to observe the interface, and a clear continuous phase. The image analysis is also always limited by the analyzing software and the ability of resolving the interface. Further, many methods require the knowledge of density of both liquids and in some cases the measurement is very difficult or even impossible if the densities are nearly equal.[20,21]

WGMs appear when light circulates in the transparent spherical object as a consequence of total internal reflection. To excite the WGMs, light is either coupled into the spherical cavity via an evanescent field or the cavity is doped with a fluorescent dye. Droplets are frequently used as WGM microcavities and lasers in various forms,[22] for example, in air,[23] on a superhydrophobic surface,[24,25] embedded in a solid,[26,27] or dispersed in another liquid.[28,29] Lasing has been also demonstrated in natural and injected droplets inside live cells.[30] In contrast to solid microcavites, the size of the droplets can be controlled extremely precisely in real time, whereas their size is monitored via WGMs.[24,29,31] Despite a wide variety of applications, WGMs in droplets have not been applied till now to measure IFT.

In this work, we demonstrate a method for measuring the IFT between two immiscible liquids by directly measuring the Laplace pressure inside the microdroplet positioned at the end of a microcapillary. WGMs in the droplet are used to measure the droplet size with nanometer precision and to simultaneously determine the refractive index of the continuous or droplet phase. The extremely high precision in combination with a 0.5 μm-wide microcapillary opening allows us to carry out measurements on very small droplets, consequently having larger Laplace pressure and larger surface-area-to-volume ratio, enabling faster equilibrium. Larger pressure is also easier to measure and some other contributions such as gravity (e.g., density difference between phases) can be neglected. The demonstrated method also enables dynamic measurements of the surfactant absorption and desorption.

2. Results and Discussion

Our new method was first used to measure IFT of a well-known hexadecane–water system.[10,17,32] The microcapillary was filled

G. Pirnat, M. Humar
Condensed Matter Department
J. Stefan Institute
Jamova 39, SI-1000 Ljubljana, Slovenia
E-mail: matjaz.humar@ijs.si

M. Humar
Faculty of Mathematics and Physics
University of Ljubljana
Jadranska 19, SI-1000 Ljubljana, Slovenia

M. Humar
CENN Nanocenter
Jamova 39, SI-1000 Ljubljana, Slovenia

The ORCID identification number(s) for the author(s) of this article can be found under https://doi.org/10.1002/adpr.202100129.

DOI: 10.1002/adpr.202100129

with hexadecane and immersed in water (**Figure 1**a). A droplet was generated at the tip of the microcapillary by applying a high pressure, typically ≈3 bar. After generation, the droplet stayed in contact with the tip of the microcapillary throughout the measurement (Figure 1b). If desired, the droplet could be easily detached from the microcapillary by shear force induced by quickly moving the microcapillary through the continuous phase. The droplet was illuminated by a green light-emitting diode (LED) or green laser to excite the fluorescent dye dissolved in the droplet phase. The generated fluorescent light was sent to a spectrometer revealing sharp spectral peaks corresponding to WGMs (Figure 1c). The peak positions were fit to the exact WGM solutions,[33] which gives any two out of the three parameters: droplet size and refractive index of the droplet phase and of continuous phase. One of these parameters must be known in advance. The smallest detectable droplet size changes were 0.02 nm, but the absolute size value was limited by the uncertainty in the refractive index. If the refractive index is known to have an accuracy of 0.001, then the absolute size uncertainty of the 30 μm droplet is 20 nm. Droplet size was typically 8–100 μm, corresponding to a volume of 2–4200 pl, enabling analysis of very small samples. The *Q*-factor of the WGMs decreases with droplet size, which ultimately limits the smallest size of the droplet. If the index difference between the inner and outer liquid is high, for example, in the case of the high-index optical oil ($n = 1.62$) and water, the smallest size is ≈8 μm. On the other end, if the droplet is too large, higher-order WGMs start to appear, which make mode identification more difficult. Also, at large droplet size, if the two liquids have significantly different densities, the droplet is more likely to detach from the microcapillary.

The droplet phase was able to freely flow between the microcapillary and the droplet, enabling the change in droplet size (Figure 1d). If the pressure in the microcapillary is equal to the Laplace pressure inside the droplet, typically in the order of 10 mbar, then there is no flow and the droplet size does not change. The condition for a stable droplet size was set at maximum WGM wavelength shift rate of 10^{-4} nm s^{-1}, which corresponds to the diameter change rate of 3×10^{-3} nm s^{-1} for a 35 μm-diameter droplet. When studying adsorption or desorption of surfactants, the maximum wavelength shift rate was set to 0.1 nm s^{-1} to enable faster measurements. In equilibrium, the IFT was simply calculated using Young–Laplace's equation $\gamma = pd/4$, where γ is the IFT, d is the droplet diameter calculated from the WGM spectrum, and p is the equilibrium pressure. The pressure was read from the pressure pump internal pressure sensor with accuracy of 0.03 mBar. As an example, for a 35 μm-diameter droplet (Figure 1d) with an equilibrium pressure of 5 mBar, the pressure reading accuracy contributes 0.6% relative error to the final IFT. No discrepancy in the equilibrium pressure value was observed whether the pressure was increased or decreased toward the equilibrium value.

To calculate the droplet size from the WGM spectrum, one refractive index, either of the droplet phase or the continuous phase, must known in advance. Indices of liquids can easily be measured by a relatively inexpensive refractometer. Even if none of the two refractive indices are known, the refractive

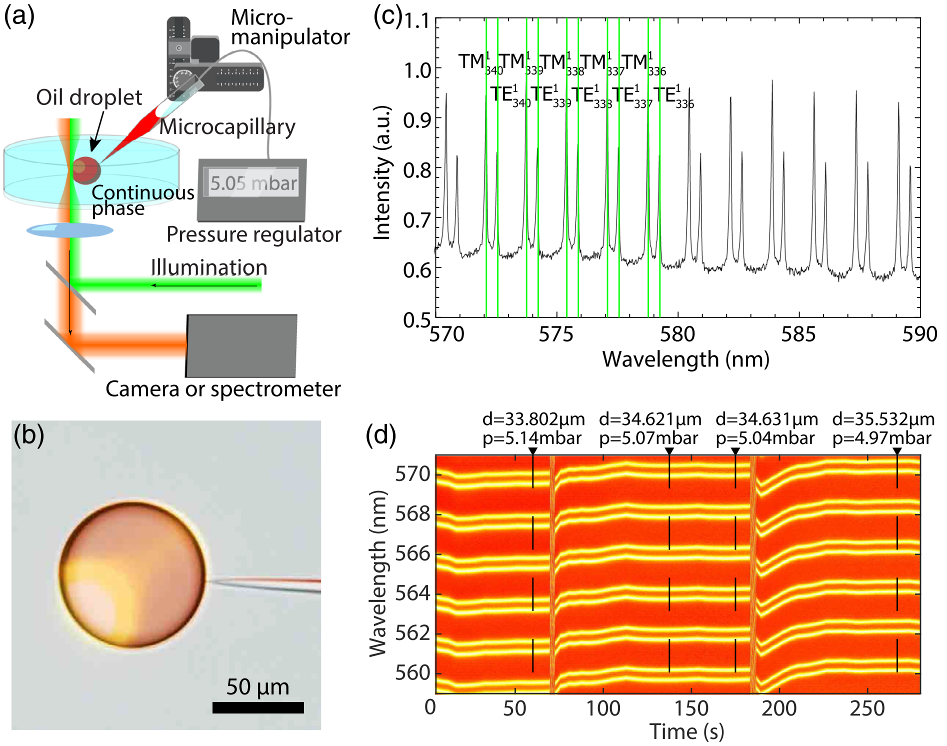

Figure 1. a) Schematic of the experimental setup, which includes a microcapillary mounted on a micromanipulator and connected to a pressure source for producing the droplets, a dish filled with the continuous phase, and an optical system for illumination and signal collection. b) Composite image (bright field and fluorescence) of a 43 μm-diameter droplet on the microcapillary end. c) Emission spectrum of the same droplet. d) WGM spectrum as the pressure inside the microcapillary is changed. Pressures and sizes at four equilibrium points are given.

indices of common liquids are in a relatively narrow range (1.33–1.50) and therefore do not have a very large effect on the measurement. Especially if one medium is water based, we can suppose it has an index close to that of pure water. Even if it is slightly different than water, for example, 1.3477 for 10% glucose, it affects the final IFT measurement by only 1%. For very precise size measurements, the chromatic dispersion of both fluids also needs to be taken into account when fitting WGMs. For hexadecane (dispersion coefficient of $-3.34 \times 10^{-5}\,\text{nm}^{-1}$ in the given wavelength range), the calculated droplet size is 3% too large if dispersion is not taken into account. If the refractive index of one phase is known precisely, then our method enables simultaneous measurement of IFT and refractive index of a very small amount of the unknown liquid. The accuracy in determining the refractive index of the continuous or droplet phase in our experiment was better than 0.002. To actually observe the WGMs, the refractive index of the droplet phase has to be larger than the continuous phase, but the refractive index difference can be as small as 0.035 for a 100 μm droplet. In rare combinations of liquids with very close refractive indices, we can still estimate the size of the droplet by optical imaging. The error of the droplet size in this case is estimated to be ≈0.3 μm which contributes 1% to the error of IFT for a 30 μm droplet. However, with optical imaging alone, it is difficult to detect small droplet diameter changes and a much longer time interval is needed to determine the equilibrium pressure. Another advantage of our method is that it can be adapted for detection though scattering layers (Figure S1, Supporting Information), due to the fact that only the spectrum is needed, which can be detected through media with high scattering.[34] There are only few other tensiometry methods that can actually measure opaque media.[17]

Droplets created by the microcapillary can be manipulated for a long period of time (tens of minutes). This allows us to study how IFT changes in time due to surfactant absorption or desorption, dissolution of one phase in another, as well as changes of IFT if the continuous phase is either slowly exchanged or some other substance is added to the continuous phase. IFT of a hexadecane droplet in pure water was measured as a function of time after the droplet was created (**Figure 2**a). During the first few minutes after droplet generation, the ITF value fell to almost half of its initial value, probably due to absorption of impurities to the droplet surface. According to the theory of dynamic adsorption for nonionic systems, Ward–Tordai's[35] model with the characteristic $\gamma(t) - \gamma_{\text{eq}} \propto t^{-1/2}$ time dependence is usually adapted,[11,36,37] where γ_{eq} is the equilibrium IFT and t is time. However, in our experiments, an exponential fit $\gamma(t) - \gamma_{\text{eq}} = Ae^{-t/\tau}$ describes our measurements better. This may be due to high curvature of the interface, which changes the absorption rate[38] and can even change the IFT value.[39] Also, other impurities in water have been shown to change the adsorption rate of the surface active molecules.[40] At this point, our goal was not to find a complete surfactant model for the particular case but to validate the accuracy of our new method. Therefore, we are interested only in the IFT value at time $t = 0$, which represents a fresh surface, and at $t \to \infty$ corresponding to an equilibrated system. When data for hexadecane droplets inside deionized water are extrapolated toward $t = 0$ (a completely fresh droplet), an IFT

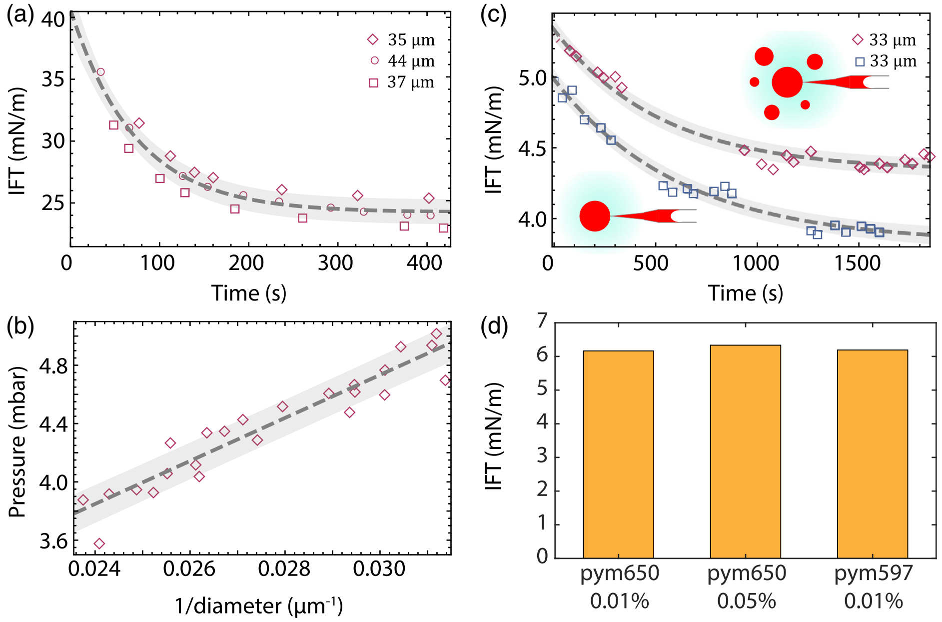

Figure 2. a) IFT time dependence for three hexadecane droplets inside pure water. Time equal to 0 corresponds to the droplet generation. Data are fit with exponential function to obtain IFT value at time zero and infinity. b) Equilibrium pressures for droplets of different diameters from 30 to 40 μm for 0.03% Span 80 in hexadecane and 0.02% Tween 20 in water. Linear dependence shows good agreement with the Young–Laplace's model. c) Difference between droplets inside pure continuous phase (blue points) and an emulsion (red points) of the same phases. IFT values for these systems are different due to surfactant partitioning. d) IFT dependence on dye and dye concentration for 0% Span 80 and 0.2% Tween system. Droplet sizes were in the range 53–65 μm.

value of $42 \pm 2\,\mathrm{mN\,m^{-1}}$ is obtained, which is in agreement with literature value of $43.16\,\mathrm{mN\,m^{-1}}$,[10,32] where ultrapure Millipore water was used. In addition, the IFT value after long time approaches $23.4 \pm 0.5\,\mathrm{mN\,m^{-1}}$, which also corresponds with literature value of $24\,\mathrm{mN\,m^{-1}}$,[17] where deionized water was used. In general, the time dependence of IFT due to surfactant molecule diffusion should be size dependant. However, because the sizes of the droplets in our experiments were in a relatively small size range (35–44 μm), no size dependence of the characteristic time is observed (Figure 2a).

Apart from the pressure provided by the pump there are also contributions from the hydrostatic pressure due to liquid height and density difference between inside and outside of the microcapillary and capillary pressure at the air–oil interface inside the microcapillary. In our setup, both of these pressure contributions are in order of $0.01 - 0.1$ mbar and act in opposite direction, so that if the microcapillary is filled to the approximate point equivalent to the capillary rise, the two pressure contributions cancel each other, resulting in an almost zero-pressure offset. Further, as the droplets are small, the typical Laplace pressure in the droplet is much larger than the pressure offset. However, for very low IFT and large droplets, the pressure offset could have a considerable effect and should be accounted for. This can be easily achieved by measuring pressure for droplets of different sizes and fitting a linear function to the resulting pressure as a function of the inverse diameter. If this pressure offset would be significant, we would expect some nonzero pressure value for a droplet of infinite size. This was tested on hexadecane–water mixture with 0.03% Span 80 in hexadecane and 0.02% Tween 20 in water (Figure 2b). Fitting to $p = 4\gamma/d + p_{\mathrm{offset}}$ gives $\gamma = 3.79 \pm 0.11\,\mathrm{mN\,m^{-1}}$ and $p_{\mathrm{offset}} = 0.3 \pm 0.3$ mbar. In this case, the offset pressure is negligible. In this case, the measured IFT value also agrees relatively well with the literature value of $4.44\,\mathrm{mN\,m^{-1}}$.[10,32] The small discrepancy could be, again, due to impurities in water and in hexadecane. The linear dependence of the pressure as the function of inverse droplet size also demonstrates that there are no differences in how differently sized droplets interact with the microcapillary. Namely, if the droplet size would be comparable with the diameter of the microcapillary, the contact angle with the microcapillary could have an effect on the measurement.

All of the earlier measurements were carried out with a single hexadecane droplet in a very large volume of the continuous phase. It is however known that the IFT can be dependent on the geometrical factor, which is defined as the total surface area of the droplets divided by volume of the continuous phase. This is due to the partitioning of surfactant molecules between the interfaces of all droplets.[13,41] Therefore, an emulsion of 0.02%v/v hexadecane in water with an average droplet size of ≈5 μm was used as the continuous phase (Figure 2c). The resulting value of $\gamma = 4.26 \pm 0.04\,\mathrm{mN\,m^{-1}}$ better matches the literature value.

As the addition of a small amount of fluorescent dye is necessary to excite the WGMs, the effects of the dye on the IFT measurement were also studied. Two different dyes (pyrromethene 597 and pyrromethene 650), the latter with two different concentrations (0.01% and 0.05%) were dissolved in hexadecane, whereas the continuous phase consisted of 0.2% Tween 20 in water. The mean IFT value across all measurements was $6.06\,\mathrm{mN\,m^{-1}}$ (Figure 2d). The largest discrepancy from the mean value is $0.13\,\mathrm{mN\,m^{-1}}$ for 0.05% of pyrromethene 650. This change is small enough that it can be neglected. Further, the WGMs are visible at even lower concentrations, where the effect of the dye is expected to be even lower.

Measurements with different liquids show that this method can be used for various liquid densities, refractive indices, and viscosities without any modification of the experimental setup. As a common liquid, sunflower oil was measured. An IFT value of $21.76 \pm 0.08\,\mathrm{mN\,m^{-1}}$ in pure water was obtained, whereas in the literature, a value of $22{-}25\,\mathrm{mN\,m^{-1}}$ is given.[42] Further, an optical oil (SL5262), which has a very high viscosity (650 cP), was measured without problem, giving $22.0 \pm 0.3\,\mathrm{mN\,m^{-1}}$. The larger error in this case is caused by higher uncertainty in the measured equilibrium pressure (70 ± 2 mbar for 12.6 μm droplet), due to higher viscosity, which reduces the responsiveness of the droplet size as the pressure changes.

3. Conclusion

In conclusion, the newly developed method enables precise IFT measurements of extremely small quantities of liquids. The setup is very simple as it requires only standard equipment, namely, a microfluidic pressure pump, microcapillary which can be purchased or made by a standard micropipette puller, an LED, or a small diode laser and a compact spectrometer. The spectrum can be captured without any sophisticated optical system, and a bare optical fiber brought close to the droplet without any lenses is sufficient. Further, no prior knowledge of the density of the liquids and the geometric properties of the measuring apparatus (e.g., micropipette size, surface properties, etc.) is needed. Refractive index of one of the liquids must be known but only very approximately. Otherwise, it can be simply measured by a refractometer. A very small size of the droplet leads to a large surface-to-volume ratio, enabling fast equilibrium with the outside medium and therefore also the study of dynamic processes such as adsorption and desorption of surfactants. The droplet size can also be quickly increased or decreased, enabling the study of redistribution of surfactant at the surface. It is also fast to make a new droplet and repeat the experiments with a different droplet size or inside another continuous phase. Even more conveniently, a standard setup for microfluidic droplet generation could be used, for example, a coflow microcapillary device, where the droplet could be generated by the microcapillary inside a microchannel.[29] The continuous phase could be changed and the time dependence of the IFT could be measured. In conclusion, the newly developed method could become a powerful technique for research as well as commercial use for a variety of liquids.

4. Experimental Section

Hexadecane (ReagentPlus 99% Sigma Aldrich, $n = 1.434$, $k_n = -3.34 \times 10^{-5}\,\mathrm{nm^{-1}}$), optical oil (Santolubes—SL5262, $n = 1.62$, $k_n = -1.0 \times 10^{-4}\,\mathrm{nm^{-1}}$), and sunflower oil ($n = 1.474$) were doped with Pyrromethene 597 or Pyrromethene 650 (Exiton). Dyes were first dissolved in acetone at 1 mg ml^{-1}, which was added to the oils and then left to evaporate to yield final dye concentrations of 0.01, 0.05, or 0.1 wt%. Deionized water (electrical conductivity ≈ 1 S cm^{-1}) was used as the continuous phase. Optionally, Span 80 (Sigma-Aldrich) and Tween 20 (Sigma-Aldrich) were dissolved at different concentrations in oils and water, respectively. Solutions were heated and stirred each time before being used. The droplets were generated by microcapillaries (Eppendorf, Femtotip II, 0.5 μm inner diameter and 0.7 μm outer diameter). The microcapillaries were treated by first filling them with hexadecane and then submerging into 0.1% solution of *N*-trimethoxysilylpropyl-*N,N,N*-trimethylammonium chloride (abcr GmbH) in water for 10 min at 60 °C. The microcapillaries were then emptied at high pressure (8 bar) and baked at 120 °C for 30 min. Microcapillaries were filled with ≈ 3 μl of the investigated oil, mounted to a micromanipulator (Eppendorf, InjectMan 4), and submerged into the continuous phase at an angle of 5−30. A clean plastic dish (a lid of an Ibidi 35 mm-diameter culture dish) was used as the container for continuous phase and was washed with ethanol, isopropyl alcohol, and deionized water before use. The sample was covered from all sides to prevent the air flow from disrupting the droplets. A high-pressure controller (Eppendorf, FemtoJet 4i, 0–8 bar) was used to initially generate a droplet. To finely control the pressure, a valve was used to switch to a more accurate and faster-response time pressure controller (Elvieflow, OB1, 0−200 mbar, 0.03 mbar accuracy). The samples were observed with an inverted microscope (Nikon Ti2) through a 20×/0.45NA objective. The droplets were illuminated by a green LED (CoolLED, pE-300) or a 532 nm continuous-wave laser with 0.5−20 mW power at the sample. The resulting fluorescent light was captured by a high-resolution spectrometer (Andor Shamrock SR-500i) at 0.06 nm spectral resolution and at 10 Hz acquisition rate.

Supporting Information

Supporting Information is available from the Wiley Online Library or from the author.

Acknowledgements

This project received funding from the European Research Council (ERC) under the European Union's Horizon 2020 research and innovation programme (grant agreement no. 851143) and from Slovenian Research Agency (ARRS) (N1-0104, J1-1697 and P1-0099).

Conflict of Interest

The authors declare no conflict of interest.

Data Availability Statement

Research data are not shared.

Keywords

droplets, interfacial tension, tensiometry, whispering gallery modes

Received: May 12, 2021
Revised: July 13, 2021

[1] R. Miller, E. Aksenenko, V. Fainerman, *Adv. Colloid Interface Sci.* **2017**, *247*, 115.
[2] L. He, F. Lin, X. Li, H. Sui, Z. Xu, *Chem. Soc. Rev.* **2015**, *44*, 5446.
[3] S. Hartland, *Surface and Interfacial Tension: Measurement, Theory, and Applications*, CRC Press, (Headquarters:) Marcel Dekker, Inc., 270 Madison Avenue, New York, NY 10016, U.S.A, **2004**.
[4] A. R. Thiam, R. V. Farese Jr., T. C. Walther, *Nat. Rev. Mol. Cell Biol.* **2013**, *14*, 775.
[5] N. Bagalkot, A. A. Hamouda, O. M. Isdahl, *MethodsX* **2018**, *5*, 676.
[6] E. Yakhshi-Tafti, R. Kumar, H. J. Cho, *Int. J. Optomechatronics* **2011**, *5*, 393.
[7] T. Kairaliyeva, E. Aksenenko, N. Mucic, A. Makievski, V. Fainerman, R. Miller, *J. Surfactants Deterg.* **2017**, *20*, 1225.
[8] J. M. Zamora, R. Marquez, A. M. Forgiarini, D. Langevin, J.-L. Salager, *J. Colloid Interface Sci.* **2018**, *519*, 27.
[9] H. H. Hu, D. D. Joseph, *J. Colloid Interface Sci.* **1994**, *162*, 331.
[10] L. W. Honaker, J. P. Lagerwall, V. Jampani, *Langmuir* **2018**, *34*, 2403.
[11] D. Needham, K. Kinoshita, A. Utoft, *Micromachines* **2019**, *10*, 105.
[12] J. L. Drury, M. Dembo, *Biophys. J.* **1999**, *76*, 110.
[13] A. Yeung, T. Dabros, J. Masliyah, J. Czarnecki, *Colloids Surf., A* **2000**, *174*, 169.
[14] R. D. Apolito, A. Perazzo, M. DAntuono, V. Preziosi, G. Tomaiuolo, R. Miller, S. Guido, *Langmuir* **2018**, *34*, 4991.
[15] A. D. Ward, M. G. Berry, C. D. Mellor, C. D. Bain, *Chem. Commun. (Cambridge, U.K.)* **2006**, *43*, 4515.
[16] J. T. Cabral, S. D. Hudson, *Lab Chip* **2006**, *6*, 427.
[17] R. Hussain, S. Vogt, A. Honari, K. Hollingsworth, A. Sederman, J. Mitchell, M. Johns, *Langmuir* **2014**, *30*, 1566.
[18] C. MacLeod, C. Radke, *J. Colloid Interface Sci.* **1993**, *160*, 435.
[19] A. Javadi, J. Krägel, P. Pandolfini, G. Loglio, V. Kovalchuk, E. Aksenenko, F. Ravera, L. Liggieri, R. Miller, *Colloids Surf., A* **2010**, *365*, 62.
[20] J.-W. Kim, H. Kim, M. Lee, J. J. Magda, *Langmuir* **2004**, *20*, 8110.
[21] M. Tintaru, R. Moldovan, T. Beica, S. Frunza, *Liq. Cryst.* **2001**, *28*, 793.
[22] D. MCGloin, *Rep. Prog. Phys.* **2017**, *80*, 054402.
[23] H. Azzouz, L. Alkhafadiji, S. Balslev, J. Johansson, N. A. Mortensen, S. Nilsson, A. Kristensen, *Opt. Express* **2006**, *14*, 4374.
[24] A. Kiraz, A. Kurt, M. Dündar, A. Demirel, *Appl. Phys. Lett.* **2006**, *89*, 081118.
[25] S. Nizamoglu, M. C. Gather, S. H. Yun, *Adv. Mater.* **2013**, *25*, 5943.
[26] V. D. Ta, R. Chen, H. D. Sun, et al., *Sci. Rep.* **2013**, *3*, 1362.
[27] M. Humar, M. Ravnik, S. Pajk, I. Muševič, *Nat. Photonics* **2009**, *3*, 595.
[28] S. K. Tang, Z. Li, A. R. Abate, J. J. Agresti, D. A. Weitz, D. Psaltis, G. M. Whitesides, *Lab Chip* **2009**, *9*, 2767.
[29] D. Richter, M. Marinčič, M. Humar, *Lab Chip* **2020**, *20*, 734.
[30] M. Humar, S. H. Yun, *Nat. Photonics* **2015**, *9*, 572.
[31] S. Yang, Y. Wang, R. Chen, T. He, H. V. Demir, H. Sun, *Sci. Rep.* **2016**, *6*, 27200.
[32] M. Hashimoto, P. Garstecki, H. A. Stone, G. M. Whitesides, *Soft Matter* **2008**, *4*, 1403.
[33] J. D. Eversole, H.-B. Lin, A. Huston, A. J. Campillo, P. T. Leung, S. Liu, K. Young, *JOSA B* **1993**, *10*, 1955.
[34] M. Humar, A. Dobravec, X. Zhao, S. H. Yun, *Optica* **2017**, *4*, 1080.
[35] A. Ward, L. Tordai, *J. Chem. Phys.* **1946**, *14*, 453.
[36] H. Diamant, D. Andelman, *J. Phys. Chem.* **1996**, *100*, 13732.
[37] K. Kinoshita, E. Parra, D. Needham, *J. Colloid Interface Sci.* **2017**, *488*, 166.
[38] X. Li, R. Shaw, G. M. Evans, P. Stevenson, *Comput. Chem. Eng.* **2010**, *34*, 146.

[39] M. D. Reichert, N. J. Alvarez, C. F. Brooks, A. M. Grillet, L. A. Mondy, S. L. Anna, L. M. Walker, *Colloids Surf., A* **2015**, *467*, 135.

[40] V. Fainerman, S. Lylyk, E. Aksenenko, N. Kovalchuk, V. Kovalchuk, J. Petkov, R. Miller, *J. Colloid Interface Sci.* **2012**, *377*, 1.

[41] V. B. Fainerman, A. A. Sharipova, S. B. Aidarova, V. I. Kovalchuk, E. V. Aksenenko, A. V. Makievski, R. Miller, *Colloids Interfaces* **2018**, *2*, 28.

[42] L. Fisher, E. Mitchell, N. Parker, *J. Food Sci.* **1985**, *50*, 1201.